AIAA 81-0602R

Flutter and Response of a Mistuned Cascade in Incompressible Flow

Krishna Rao V. Kaza*
University of Toledo, Toledo, Ohio
and
NASA Lewis Research Center, Cleveland, Ohio
and
Robert E. Kielb†
NASA Lewis Research Center, Cleveland, Ohio

This paper presents an investigation of the effects of blade mistuning on the aeroelastic stability and response of a cascade in incompressible flow. The aerodynamic, inertial, and structural coupling between the bending and torsional motions of each blade and the aerodynamic coupling between the blades are included in the formulation. A digital computer program was developed to conduct parametric studies. Results indicate that the mistuning has a beneficial effect on the coupled bending-torsion and uncoupled torsion flutter. The effect of mistuning on forced response, however, may be either beneficial or adverse, depending on the engine order of the forcing function. Additionally, the results illustrate that it may be feasible to utilize mistuning as a passive control to increase flutter speed while maintaining forced response at an acceptable level.

Nomenclature

$[A]$ = aerodynamic matrix due to motion
$[A_r]$ = aerodynamic matrix due to motion in rth mode, $r=0, 1, 2 \ldots N-1$
$\{AD\}$ = aerodynamic matrix due to wake-induced flow
$\{AD_r\}$ = aerodynamic matrix due to wake-induced flow in the rth mode, $r=0, 1, 2 \ldots N-1$
a = elastic axis location, nondimensional
b = semichord
c = chord
$[D], [D_s]$ = matrices defined in Eq. (9), $s=0, 1, 2 \ldots N-1$
$[E]$ = matrix defined in Eq. (4)
$E(s,r)$ = defined in Eq. (4)
e = base for natural logarithm
$[G], [G_s]$ = matrices defined in Eq. (9), $s=0, 1, 2 \ldots N-1$
$G_{Kh_s}, G_{K\alpha_s}$ = quantities defined in Eq. (9)
h_s = amplitude of bending deflection of sth blade
h_{ar} = amplitude of bending deflection of blade in rth mode of tuned cascade
$[I]$ = unit matrix
I_{α_s} = mass moment of inertia of sth blade about elastic axis per unit span ($=m_s r_{\alpha_s}^2 b^2$)
i = $\sqrt{-1}$
K_{h_s}, K_{α_s} = bending and torsional stiffness, respectively, of sth blade
k = reduced frequency, $\omega b/V$
k_F = reduced flutter frequency, $\omega_F b/V_F$
L_s^M, L_s^w = lift due to motion and wake, respectively, of sth blade per unit span, positive up
$\ell_{hhr}, \ell_{h\alpha r}$ = nondimensional lift coefficients due to bending and torsional motions, respectively, in rth mode
$\ell_{\alpha hr}, \ell_{\alpha\alpha r}$ = nondimensional moment coefficients due to bending and torsional motions, respectively, in rth mode
$\ell_{whr}, \ell_{w\alpha r}$ = nondimensional lift and moment coefficients, respectively, due to wake in rth mode
M_s^M, M_s^w = moment about the elastic axis due to motion and wake, respectively, of sth blade per unit span, positive nose up
m_s = mass per unit span of sth blade
N = number of blades in cascade
$[P]$ = matrix defined in Eq. (9)
r = integer specifying the mode of tuned rotor, $r=0, 1, 2 \ldots N-1$; also the engine order of the excitation
r_{α_s} = radius of gyration of sth blade, nondimensionalized with respect to b
s = integer specifying blade, $s=0, 1, 2 \ldots N-1$; also blade spacing (Fig. 1)
S_{α_s} = static mass moment of sth blade per unit span about elastic axis, positive when center of gravity is aft of elastic axis
t = time
V = freestream velocity relative to the blade
V_F = flutter speed
w_r = velocity induced by wakes
$\{X\}$ = column matrix, defined in Eq. (4)
X, Z = rectangular coordinate axes
x_{α_s} = dimensionless static unbalance of sth blade ($=S_{\alpha_s}/m_s b$)
$\{Y\}$ = column matrix, defined in Eq. (4)
α_s = amplitude of torsional motion of sth blade, positive clockwise
$\alpha_{s,id}$ = torsional amplitude of each blade of tuned rotor
α_{ar} = amplitude of torsional deflection of a blade in rth mode of a tuned cascade
β_r = interblade phase angle, $2\pi r/N$
γ = nondimensional eigenvalue, $(\omega_0/\omega)^2$
γ_{h_s} = nondimensional uncoupled bending frequency of sth blade
γ_{α_s} = nondimensional uncoupled torsional frequency of sth blade
$\zeta_{h_s}, \zeta_{\alpha_s}$ = damping ratios of sth blade in bending and torsion, respectively
η = location of elastic axis measured from leading edge, $(a+1)/2$

Presented as Paper 81-0602 at the AIAA/ASME/ASCE/AHS 22nd Structures, Structural Dynamics and Materials Conference, Atlanta, Ga., April 6-8, 1981; submitted April 24, 1981; revision received Dec. 7, 1981.

*Adjunct Professor, Mechanical Engineering Department. Associate Fellow AIAA.
†Aerospace Engineer, Structures Branch. Member AIAA.

μ_s = mass ratio of sth blade, $m_s/\pi\rho b^2$
$\bar{\mu}$ = real part of eigenvalue, defined in Eq. (10)
$\bar{\nu}$ = imaginary part of eigenvalue, defined in Eq. (10)
$\bar{\nu}_F$ = nondimensional flutter frequency
ξ = stagger angle, Fig. 1
ρ = fluid density
ω = frequency
ω_0 = reference frequency
ω_{h_s} = $\sqrt{K_{h_s}/m_s}$
ω_{α_s} = $\sqrt{K_{\alpha_s}/I_{\alpha_s}}$
$[\ ],\{\ \}$ = matrices
$(\ )$ = differentiation with time
$[\ ]^{-1}$ = inverse of a matrix
Σ = indicate summation over $r=0, 1, 2 \ldots N-1$

Introduction

IN the development of modern aircraft turbofan engines, the aeroelastic stability and response of bladed-disk assemblies have been among the most difficult problems encountered. The study of stability and response in these assemblies is complicated by the presence of small differences between the individual blades, known as mistuning. The published results in this area which will be discussed later have shown that mistuning can have a beneficial effect on turbine engine blade flutter and an adverse effect on forced response. Experience[1,2] has further shown that there have been costly failures in the development and production phases in which mistuning appeared to have played an important role. Thus, an improved basic understanding of these effects is important in the design phase.

To improve the basic understanding of the effects of mistuning on aeroelastic stability and response and then to explore the possibility of utilizing mistuning as a passive control to alleviate flutter and to minimize forced response, an effort has been in progress at the NASA Lewis Research Center. As a part of this general effort, the effects of mistuning on coupled bending-torsion flutter and on aeroelastic response due to wakes have been studied. This paper presents the results of the study for incompressible flow.

Either because of the complexities or because of the general belief that the turbomachinery blade flutter involves only a single degree of freedom, previous researchers[2-7] have studied the effect of blade mistuning on aeroelastic stability and response by considering either pure bending motion or pure torsional motion of the blades. The studies of multidegree-of-freedom blade flutter in the published literature[5,8-11] have been limited to tuned cascades. To the best of the authors' knowledge, the forced response of both tuned and mistuned cascades using multidegree-of-freedom models has not been presented in the published literature. Thus, the problem considered in this paper is a logical extension to the present state of the literature of flutter and forced response of blades with mistuning.

The mathematical model considered herein is of the discretized, lumped parameter type, utilizing discrete masses, mass moment of inertia, and linear and rotational springs to represent the individual blades. The unsteady aerodynamic loads were calculated by using Whitehead's[12] incompressible flow cascade theory. Thus, the model considered is simple enough to be used for extensive parametric studies. At the same time, it is adequate to represent the basic dynamic characteristics of a mistuned cascade, to provide guidance in refining both the aerodynamic and structural models, and to check the results obtained from finite-element formulations, such as the one presented in Ref. 13. Recently, the authors extended the present work into the subsonic and supersonic flow regimes in Ref. 14.

Theory

In general, the components which comprise a bladed-disk system have complex geometries. To accomplish the stated objectives of the paper, it is necessary to develop a model which simplifies the analysis, yet maintains the basic dynamic characteristics. For this reason only two degrees of freedom (one bending and one torsion) for each blade are considered in this paper. However, the authors have plans to add additional blade degrees of freedom and disk flexibilities in addition to other refinements to the present model. The general motion of a mistuned cascade is assumed to be a combination of all possible motions of the associated tuned cascade. It will, therefore, be instructive first to develop and understand the model of a tuned cascade.

Tuned Cascade Model

The geometry of a tuned cascade model is shown in Fig. 1. The disk is assumed to be rigid and the bladed assembly is modeled as an infinite two-dimensional cascade of airfoils in a uniform upstream flow with a velocity V as illustrated in Fig. 1. The effects of wakes shed from upstream obstructions are included. The wakes considered are limited to sinusoidal distortions represented by vorticity perturbation, so that they are convected downstream at the flow velocity V. The amplitude of the wakes is specified by the velocity which the wakes would induce at the position of the midchord point of the reference blade as indicated in Fig. 1. The motion of the airfoils in each mode of the tuned cascade is assumed to be simple harmonic with a constant phase angle β_r between adjacent blades. Also, this interblade phase angle is restricted by Lane's[15] assumption to the N discrete values $\beta_r = 2\pi r/N$ where $r=0, 1, 2 \ldots N-1$. Consequently, there are N modes for the cascade with each blade having the same amplitude. The motion of a tuned cascade in the rth mode involving bending and torsion coupling can be represented in the form of a traveling wave as shown in Fig. 1. For a tuned system, the modes with different interblade phase angles are uncoupled and hence one can write

$$\begin{Bmatrix} h_s/b \\ \alpha_s \end{Bmatrix} e^{i\omega t} = \begin{Bmatrix} h_{ar}/b \\ \alpha_{ar} \end{Bmatrix} e^{i(\omega t + \beta_r s)} \qquad (1)$$

Furthermore, it is adequate to analyze the motion of a single blade in each of the interblade phase angle modes separately. Hence, the number of degrees of freedom of a tuned cascade for the present case is reduced to two for each value of β_r.

Mistuned Cascade Model

In a randomly mistuned cascade, the blades are not identical and can have different response amplitudes. In addition, the phase angle between adjacent blades can vary.

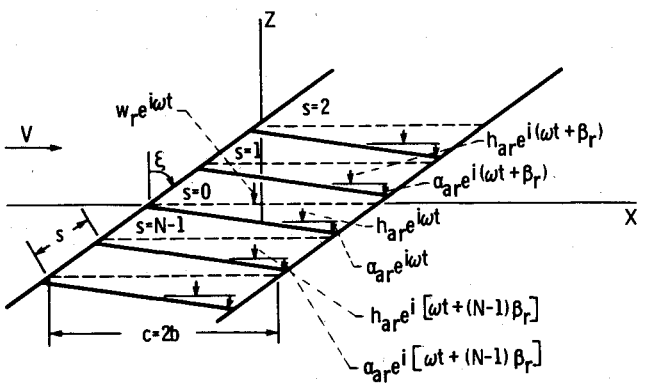

Fig. 1 Geometry of a tuned cascade in rth mode (note that the variable s represents the gap between the chords as well as the blade number index).

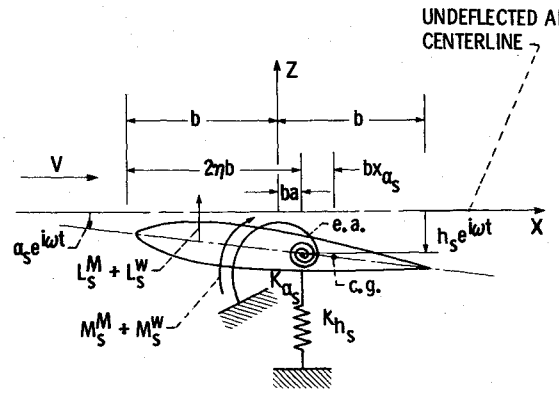

Fig. 2 Airfoil restrained from bending and torsional motion (sinusoidal wakes not shown).

Table 1 Parameters of NASA test rotor 12

N	56
s/c	0.534
μ_s	258.5
a	0 (varied in some cases)
x_{α_s}	0 (varied in some cases)
r_{α_s}	0.5774 ($a=0$)
	0.7638 ($a=-0.5$ and 0.5)
ξ	54.4 deg
$\omega_{h_s}/\omega_{\alpha_s}$ (tuned)	0.357 (varied in some cases)

Because of the spatial periodicity, the general motion of a blade in a mistuned cascade can be expressed as a combination of the motions in all possible interblade phase angle modes of the corresponding tuned cascade. Consequently, the motion of the sth blade can be written in the traveling wave form

$$\begin{Bmatrix} h_s/b \\ \alpha_s \end{Bmatrix} e^{i\omega t} = \sum_{r=0}^{N-1} \begin{Bmatrix} h_{ar}/b \\ \alpha_{ar} \end{Bmatrix} e^{i(\omega t + \beta_r s)} \tag{2}$$

The quantities h_{ar} and α_{ar} were called the "aerodynamic modes" in Ref. 4. For a cascade with N mistuned blades, Eq. (2) can be generalized as

$$\{X\}e^{i\omega t} = [E]\{Y\}e^{i\omega t} \tag{3}$$

where

$$\{X\} = \begin{Bmatrix} h_0/b \\ \alpha_0 \\ \cdot \\ \cdot \\ \cdot \\ h_{N-1}/b \\ \alpha_{N-1} \end{Bmatrix} \quad \{Y\} = \begin{Bmatrix} h_{a0}/b \\ \alpha_{a0} \\ \cdot \\ \cdot \\ \cdot \\ h_{a(N-1)}/b \\ \alpha_{a(N-1)} \end{Bmatrix}$$

$$[E] = \begin{bmatrix} E(0,0) & 0 & E(0,1) & 0 & \cdots \\ 0 & E(0,0) & 0 & E(0,1) & \cdots \\ E(1,0) & 0 & \cdots & & \\ 0 & E(1,0) & \cdots & & \\ \vdots & \vdots & & E(N-1,N-1) & 0 \\ & & & 0 & E(N-1,N-1) \end{bmatrix} \tag{4}$$

$$E(s,r) = e^{2\pi i s r/N}$$

It should be remarked that the motion of a blade in a cascade with and without mistuning can also be expressed in a standing wave form. An interesting discussion on both traveling and standing wave representations for tuned bladed-disk assemblies is presented in Ref. 16.

Structural Model

The structural model of the sth blade of a mistuned cascade is illustrated in Fig. 2. Each airfoil is suspended by bending and torsional springs, K_{h_s} and K_{α_s}, respectively. The airfoil is assumed to be rigid in the chordwise direction, and this motion is neglected. The elastic coupling between bending and torsion due to pretwist, shrouds, and rotation of the rotor could also be modeled through the offset distance between the center of gravity and elastic axis. The centrifugal stiffening effects due to rotation are included in the bending and torsional spring constants. The elastic and dynamic properties of the blades are represented by their respective values at the three-quarters station of blade span. This model may be viewed as a logical extension of the so-called "typical section wing" used in fixed-wing aeroelasticity.[17]

Aerodynamic Model

The unsteady aerodynamic loads were calculated by using Whitehead's[12] cascade theory in the incompressible unsteady flow. This theory is an extension of two-dimensional unsteady airfoil theory of Theoderson to account for cascade effects. The effect of airfoil thickness, camber, and steady-state angle of attack are neglected. As mentioned earlier, the effects of wakes from a periodic obstruction upstream are included in the form of a vorticity perturbation. It should be noted that the direction of the velocity, as shown in Fig. 1, induced by the wakes is opposite to that of Ref. 12. In view of the basic objectives of this paper, it is felt that this incompressible theory is adequate. However, the compressibility effects by using Smith's[18] theory in the subsonic flow regime and Adamczyk and Goldstein's[19] theory in the supersonic flow regime are included in Ref. 14.

Equations of Motion

A simple application of Lagrange's equation to the mathematical model of the sth blade in Fig. 2 leads to the following coupled bending-torsion equations:

$$\begin{bmatrix} m_s & S_{\alpha_s} \\ S_{\alpha_s} & I_{\alpha_s} \end{bmatrix} \begin{Bmatrix} \frac{d^2}{dt^2}(h_s e^{i\omega t}) \\ \frac{d^2}{dt^2}(\alpha_s e^{i\omega t}) \end{Bmatrix} + \begin{bmatrix} (1+2i\zeta_{h_s}) m_s \omega_{h_s}^2 & 0 \\ 0 & (1+2i\zeta_{\alpha_s}) I_{\alpha_s} \omega_{\alpha_s}^2 \end{bmatrix} \times \begin{Bmatrix} h_s e^{i\omega t} \\ \alpha_s e^{i\omega t} \end{Bmatrix} = \begin{Bmatrix} -L_s^M - L_s^w \\ M_s^M + M_s^w \end{Bmatrix} \tag{5}$$

Structural damping is added to the equations of motion by multiplying the uncoupled stiffness coefficients in the bending and torsion by $(1+2i\zeta_{h_s})$ and $(1+2i\zeta_{\alpha_s})$, respectively. The aerodynamic forces due to motion, represented by the superscript M, and due to excitation from sinusoidal wakes, represented by the superscript w, are expressed in terms of nondimensional coefficients as follows:

$$L_s^M + L_s^w = -\pi\rho b^3\omega^2 \sum_{r=0}^{N-1} \left[\ell_{hhr}\frac{h_{ar}}{b} + \ell_{h\alpha r}\alpha_{ar} + \ell_{whr}\right] e^{i(\omega t+\beta_r s)} \quad (6a)$$

$$M_s^M + M_s^w = \pi\rho b^4\omega^2 \sum_{r=0}^{N-1} \left[\ell_{\alpha hr}\frac{h_{ar}}{b} + \ell_{\alpha\alpha r}\alpha_{ar} + \ell_{w\alpha r}\right] e^{i(\omega t+\beta_r s)} \quad (6b)$$

$$\ell_{hhr} = \frac{2i}{k}(C_{Fq})_\eta \qquad \ell_{\alpha\alpha r} = \frac{4}{k^2}(C_{M\alpha})_\eta$$

$$\ell_{h\alpha r} = \frac{2}{k^2}(C_{F\alpha})_\eta \qquad \ell_{w\alpha r} = \frac{-4w_r}{k^2 V}(C_{Mw})_\eta$$

$$\ell_{whr} = \frac{-2w_r(C_{Fw})_\eta}{k^2 V} \qquad k = \frac{\omega b}{V}$$

$$\ell_{\alpha hr} = \frac{4i}{k}(C_{Mq})_\eta \quad (7)$$

The coefficients $(C_{Fq})_\eta$, $(C_{F\alpha})_\eta$ ... $(C_{Mw})_\eta$ are calculated by the unsteady cascade airfoil theory of Reference 12 for given values of k, b, s/c, ξ, and $a\,(=2\eta-1)$. The quantity w_r is the amplitude of the velocity of the sinusoidal wake in the rth mode. Nondimensionalizing Eq. (5), extending the resultant equation to all the blades ($s=0, 1, 2 \ldots N-1$), and using Eq. (3), the equations for all the blades of a randomly mistuned cascade can be simplified as

$$[[P]-[I]\gamma]\{Y\} = -[E]^{-1}[G][E]\{AD\} \quad (8)$$

where

$$[P] = [[E]^{-1}[D][E] + [E]^{-1}[G][E][A]]$$

$$[D] = \begin{bmatrix} [D_0] & & & \\ & [D_1] & & \\ & & \ddots & \\ & & & [D_{N-1}] \end{bmatrix} \quad G_{Kh_s} = \mu_s\gamma_{h_s}^2(1+2i\zeta_{h_s}) \quad G_{K\alpha_s} = \mu_s r_{\alpha_s}^2\gamma_{\alpha_s}^2(1+2i\zeta_{\alpha_s})$$

$$[G] = \begin{bmatrix} [G_0] & & & \\ & [G_1] & & \\ & & \ddots & \\ & & & [G_{N-1}] \end{bmatrix} \quad \gamma_{h_s} = \omega_{h_s}/\omega_0 \quad \gamma_{\alpha_s} = \omega_{\alpha_s}/\omega_0$$

$$[A] = \begin{bmatrix} [A_0] & & & \\ & [A_1] & & \\ & & \ddots & \\ & & & [A_{N-1}] \end{bmatrix} \quad \mu_s = m_s/\pi\rho b^2$$

$$\{AD\} = [\{AD_0\}\{AD_1\}\cdots\{AD_{N-1}\}]^T \quad r_{\alpha_s}^2 = I_{\alpha_s}/m_s b^2$$

$$[D_s] = \mu_s \begin{bmatrix} 1/G_{Kh_s} & x_{\alpha_s}/G_{Kh_s} \\ x_{\alpha_s}/G_{K\alpha_s} & r_\alpha^2/G_{K\alpha_s} \end{bmatrix} \quad x_{\alpha_s} = S_{\alpha_s}/m_s b \quad \gamma = (\omega_0/\omega)^2$$

$$[A_r] = \begin{bmatrix} \ell_{hhr} & \ell_{h\alpha r} \\ \ell_{\alpha hr} & \ell_{\alpha\alpha r} \end{bmatrix} \quad \{AD_r\} = [\ \ell_{whr} \quad \ell_{\omega\alpha r}\ ]^T$$

$$[G_s] = \begin{bmatrix} 1/G_{Kh_s} & 0 \\ 0 & 1/G_{K\alpha_s} \end{bmatrix} \quad (9)$$

Solution

The aeroelastic stability of the cascade is determined by eigenvalues γ of the matrix $[P]$. The relation between the frequency ω and γ is

$$i\omega/\omega_0 = i/\sqrt{\gamma} = \bar{\mu} \pm i\bar{\nu} \quad (10)$$

Flutter occurs when $\bar{\mu} > 0$.

For the given value of the number of blades, and hence the allowable interblade phase angles, the gap-to-chord ratio, the stagger angle, the elastic axis position, and the structural parameters, the eigenvalues of the matrix $[P]$ are calculated for a range of values of k. Denoting the values of k and $\bar{\nu}$ at which $\bar{\mu}=0$ as k_F and $\bar{\nu}_F$, respectively, the nondimensional flutter speed can be written as

$$V_F/b\omega_0 = \bar{\nu}_F/k_F \quad (11)$$

The aeroelastic response of the blades induced by wakes is calculated from Eq. (8) and is

$$\{Y\} = -[[P]-[I]\gamma]^{-1}[E]^{-1}[G][E]\{AD\} \quad (12)$$

The amplitude of each blade is obtained by substituting Eq. (12) into Eq. (3).

Results and Discussion

Computer Program

A digital computer program was written to calculate the flutter stability boundaries and the blade response of a randomly mistuned rotor. In this program, it is possible to consider any type of mistuning such as blade-to-blade variations of the uncoupled bending and torsional frequencies, damping ratios, mass ratios, elastic axis and center of gravity positions, and so on. This program is operational on the NASA Lewis Research Center IBM 370/3033. Both tuned and mistuned uncoupled bending and uncoupled torsion cases, in addition to the tuned coupled bending-torsion case, can be treated as special cases of this program.

Aeroelastic Stability

A compressor stage representative of a forward stage of an advanced axial flow compressor was chosen for conducting parametric studies. This stage, known as the NASA test rotor 12, is shown in Fig. 3. The required parameters of this stage were calculated from the data given in Ref. 20 and are listed in Table 1. The ratio of blade bending to torsion frequency for this rotor is 0.357, and the elastic axis and c.g. position are at 50% chord. As a result, the coupling between bending and torsion is very weak and the flutter mode is dominated by torsional motion. Hence, the results for the predominantly bending modes for some cases will not be presented. However, to conduct parametric studies the bending-to-torsion-frequency ratio and elastic axis position are varied. For these cases the results for predominantly bending modes are included. In some selected cases only coupled torsional motion is considered.

A comparison of the system eigenvalues of both tuned and mistuned cascades is useful to understand the mistuning effects. For example, Fig. 4 is such a plot for a special case in which only uncoupled torsional motion of the blades is considered. The first type of mistuning considered is the one in which the odd and even numbered blades have different torsional frequencies. This is known as alternate blade mistuning. For example, in the case of 1% mistuning, the frequency ratio $\omega_{\alpha_s}/\omega_0$ is 1.005 for all the even blades and is 0.995 for all the odd blades. The reference frequency ω_0 is equal to the arithmetic mean of the uncoupled torsional frequencies of all the blades. Because of the symmetry of this type of mistuning the β_r mode couples with the $(\beta_r+\pi)$ mode

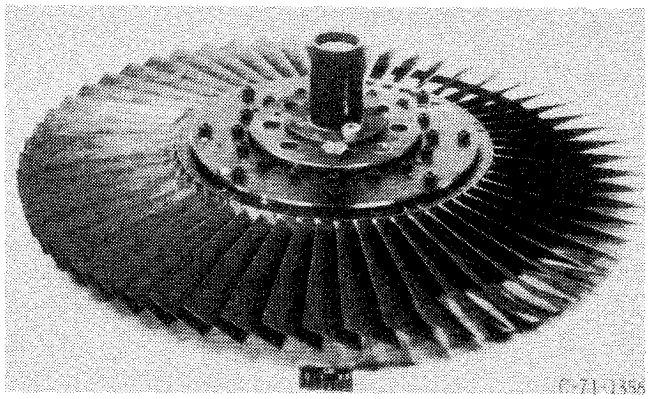

Fig. 3 NASA test rotor 12.

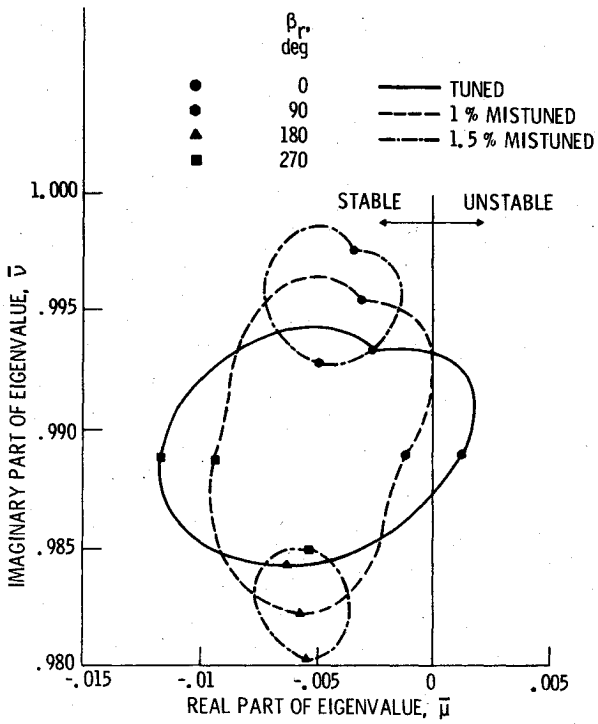

Fig. 4 Effect of alternating blade mistuning on eigenvalues (torsion only): $a=0$, $k=0.642$, $\zeta_{h_s}=\zeta_{\alpha_s}=0$.

only. Figure 4 may be viewed as a root locus for the tuned cascade with β_r as the parameter. When the blades are mistuned, this description is not completely appropriate because each mode contains all of the possible interblade phase angles. Due to the inherent symmetry in alternate blade mistuning, each mistuned mode contains only two interblade phase angle modes. However, one can view this plot as a root locus with a predominant interblade phase angle as a parameter.

Several interesting observations follow from Fig. 4. Even 1% of mistuning significantly affected the system eigenvalues and stabilized an unstable tuned cascade. As the level of mistuning is increased, the horizontal width of the root locus is decreased. This amounts to saying that the effective damping of some modes is increased while that of others is decreased. This behavior will have an influence on forced response which will be discussed later. When the mistuning level is 1.5%, the root locus is split into high- and low-frequency groups. In the high-frequency group all the interblade phase angles between 0 and 90 deg and between 276.4 and 360 deg are predominant; in the low-frequency group those between 96.4 and 270 deg are predominant. As the level

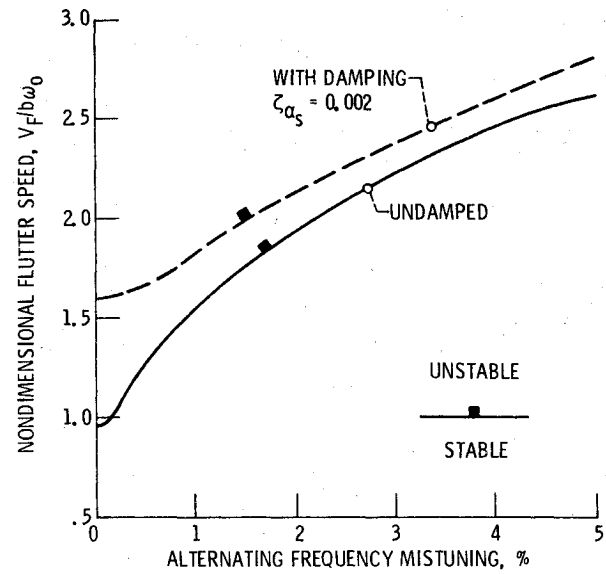

Fig. 5 Variation of uncoupled torsional flutter speed with alternating blade mistuning both with and without damping; $a=0$.

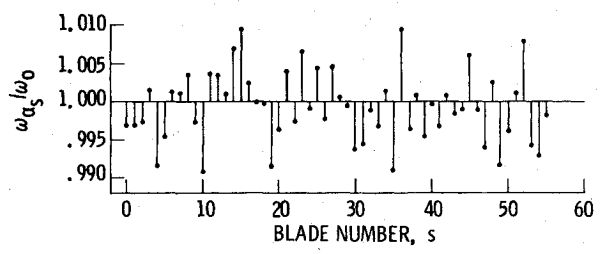

Fig. 6 Individual blade torsional frequencies for the randomly mistuned case.

of mistuning is increased beyond 1.5%, the frequency separation of these groups becomes larger and the area enclosed by each group decreases.

Figure 5 illustrates the variation of uncoupled flutter speed with the level of alternating blade mistuning with and without damping. The value of the damping ratio used is 0.2% and is the same for all the blades. The results indicate that the mistuning has a substantial effect on flutter speed. For the undamped case, the flutter speed increases monotonically with the increase in mistuning level. However, when the mistuning level is 5% and more, the additional benefit is modest. For the damped case a similar variation in flutter speed is noticed, except when the mistuning is between 0-1%. In this range, the damping effect is more pronounced. It should be noted that these observations, particularly the effects of mistuning, are in agreement with the qualitative conclusions analytically reached in Ref. 4 and the experimental results reported in Ref. 21.

A second, more common type of mistuning was analyzed. Blade torsional frequencies were randomly chosen from a normally distributed population with a mean $\omega_{\alpha_s}/\omega_0$ of 1 and a standard deviation of 0.005. The resulting blade frequencies are shown in Fig. 6. A comparison of both the tuned and mistuned eigenvalues is shown in Fig. 7. The tuned eigenvalues are the same as those presented in Fig. 4. As can be seen, there is a stabilizing effect on the system, but it is not quite as strong as that produced by 1% alternating mistuning shown in Fig. 4. The eigenvector for the least stable mode shows that each blade has a different amplitude and the interblade phase angle varies considerably. Furthermore, it was noticed that this mode involves only a localized phenomenon since only blades 42-51 have large amplitudes. This type of behavior has been observed in actual engine tests.

The effect of elastic axis position on flutter speed is of interest. Both uncoupled torsional and coupled bending-torsion flutter analyses were performed with and without damping for three elastic axis positions with the center of gravity at midchord. As was noticed in Ref. 11, very weak instabilities appeared in some cases which were eliminated by the addition of a small amount of structural damping. Consequently, they are of little practical interest and, hence, only the results with structural damping are presented in Fig. 8. Note that for uncoupled torsional flutter the worst location of the elastic axis is at the midchord point ($a=0$). This is in contrast to the present results (although not shown) without damping and to those in Refs. 3 and 11 in which a severe drop in flutter speed is noticed for the 75% elastic axis position. For coupled bending-torsion flutter, the effect of elastic axis position depends on ω_{h_s}/ω_0. If $\omega_{h_s}/\omega_0<1$, the best location (of the three locations investigated herein) is the 75% chord point; if $\omega_{h_s}/\omega_0>1$, the best location is the 25% chord point. When the elastic axis is off the midchord, the effect of bending-torsion coupling on flutter speed is significant. This observation is in agreement with that in Refs. 5 and 11. These results suggest that the tailoring of the elastic axis position can be used as a passive control to increase flutter speed as is done in fixed-wing aeroelasticity.

Figure 9 shows the effects of both alternating blade mistuning and damping on coupled bending-torsion flutter speed. As can be seen, both mistuning and damping have beneficial effects. However, the level of benefit depends on ω_{h_s}/ω_0. It should be noted that the adverse effect of coupling between bending and torsion on the tuned cascade flutter speed when $\omega_{h_s}/\omega_0<1$ is reduced by the beneficial effect of small mistuning and/or damping.

The effects of alternating blade mistuning, damping, and elastic axis position on the coupled bending-torsion flutter speed are illustrated in Fig. 10. The effects of mistuning and damping are similar to those discussed in Fig. 5; the effects of the elastic axis position are similar to those discussed in Fig. 8. Hence, one can conclude that the mistuning also has a beneficial effect on coupled bending-torsion flutter speed when the elastic axis is off the midcord.

Aeroelastic Response

In the present formulation, it is possible to consider an excitation function consisting of all harmonics of rotational speed of the rotor which range up to $r=N-1$. In engine aeroelastic terminology, the harmonic number r is known as the "engine order" of the excitation. The coefficients ℓ_{whr} and ℓ_{war} in Eqs. (6) represent the forcing functions in the bending and torsion equations, respectively. To understand the nature of the response, excitation in only one harmonic at a time will be considered. This results in no loss of generality since the principle of superposition holds. If the $r=R$ harmonic is considered, then the column matrices $\{AD_0\}$, $\{AD_1\}$, ..., $\{AD_{N-1}\}$ are zero [except (AD_R)] in Eq. (9). According to the traveling wave representation in Fig. 1, this corresponds to the case in which there are $(N-R)$ symmetrically spaced obstructions located upstream from the blades and the circumferential wake distribution is perfectly sinusoidal. For practical applications, the forcing frequency is thus equal to $(N-R)$ times the rotational speed.

The aeroelastic response results presented herein are for two values of R, 11 and 39, at a fixed reduced frequency

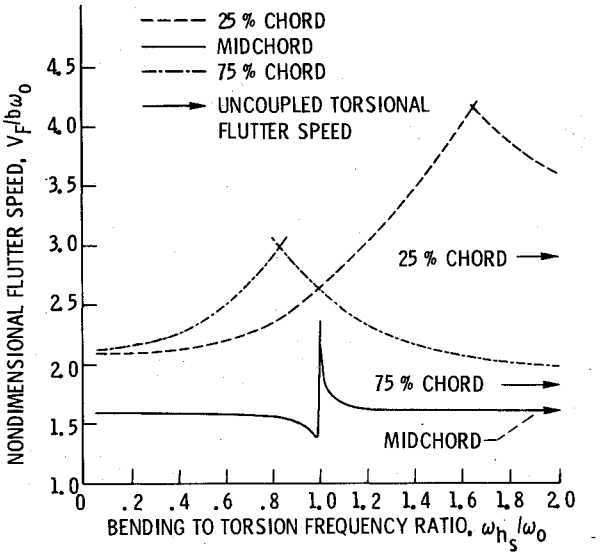

Fig. 8 Effect of bending-torsion coupling on flutter speed: $\zeta_{h_s}=\zeta_{\alpha_s}=0.002$, c.g. at midchord.

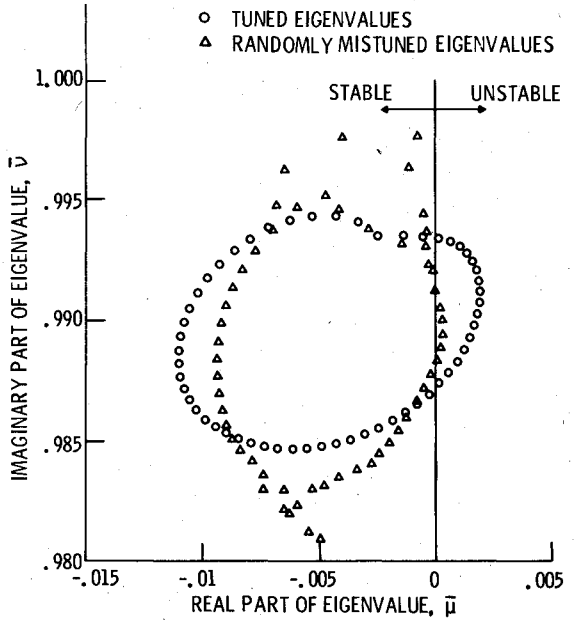

Fig. 7 Effect of random mistuning on eigenvalues (torsion only): $a=0$, $k=0.642$, $\zeta_{h_s}=\zeta_{\alpha_s}=0$.

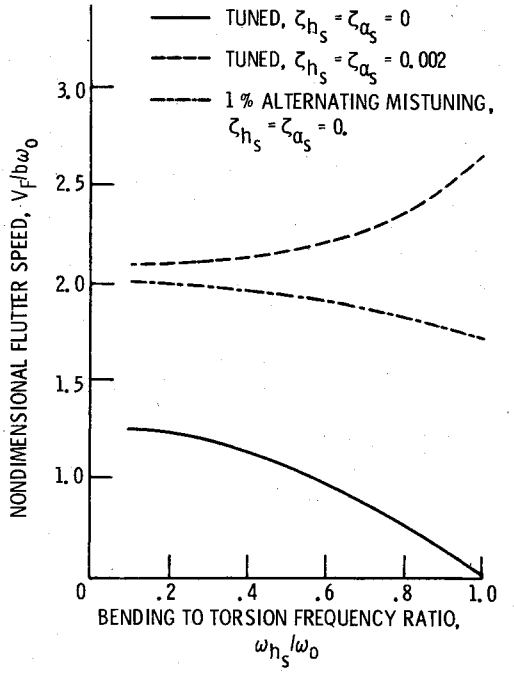

Fig. 9 Effect of mistuning and structural damping on coupled bending-torsion flutter: $a=-0.5$, c.g. at midchord.

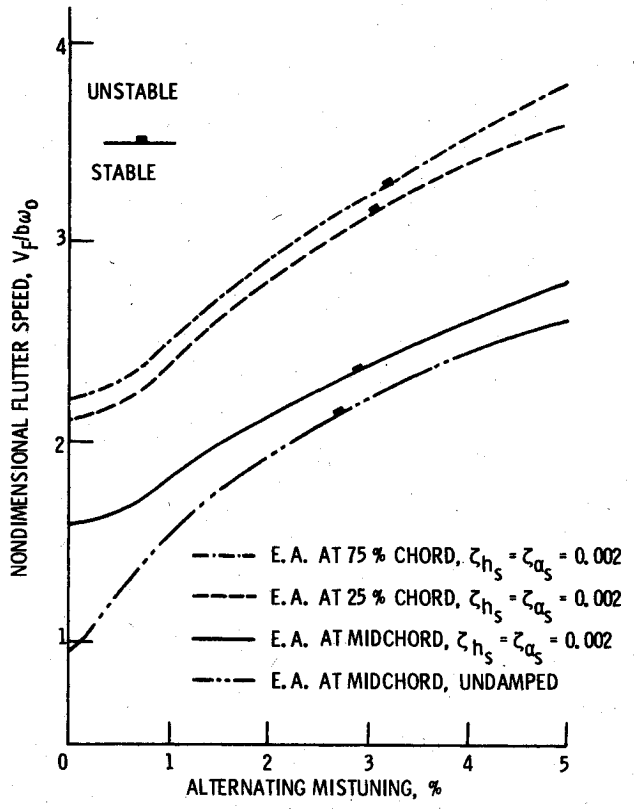

Fig. 10 Variation of coupled bending-torsion flutter speed with mistuning: $\omega_{h_s}/\omega_0 = 0.357$, c.g. at midchord.

chosen such that the cascade is aeroelastically stable in all modes. These values for R were picked because the aerodynamic damping of the tuned system in the $r = 11$ mode is relatively low, whereas that in the $r = 39$ mode is relatively high. The forcing frequency range investigated is limited to a small range around the uncoupled torsional frequency.

If the blades are tuned, the response will be entirely in the $r = R$ mode, and all the blades have equal amplitude, which is a function of ω/ω_0. Let the torsional amplitude of resonance of each blade of the tuned rotor be $\alpha_{s,id}$. If the blades are now randomly mistuned, there will be a response in all the modes (enumerated by r) and the amplitude of response of the sth blade is

$$\begin{Bmatrix} h_s/b \\ \alpha_s \end{Bmatrix} = \sum_{r=0}^{N-1} \begin{Bmatrix} h_{ar}/b \\ \alpha_{ar} \end{Bmatrix} e^{i\beta_r s} \qquad (13)$$

Figure 11 with $R = 11$ and 39 shows the variation of $\alpha_s/\alpha_{s,id}$ for both the tuned and 1% alternating blade mistuned cascades.

Note that the torsional amplitude $\alpha_{s,id}$ of the tuned cascade depends on the level of damping and R. The bending amplitudes are not shown because they are very small in the range of the excitation frequency shown herein. For the alternating blade mistuning, only two r modes are coupled and the amplitudes of the odd and even blades are different. As a result, the single resonance peak of the tuned cascade is replaced by twin resonance peaks for the alternating mistuned cascade. It is seen that the effect of mistuning on forced response depends on the engine order of the forcing function. For example, the mistuning has a beneficial effect (Fig. 11a) on torsional response for $R = 11$, but has an adverse effect (Fig. 11b) for $R = 39$. This is in contrast to the common belief that the mistuning always has an adverse effect on forced

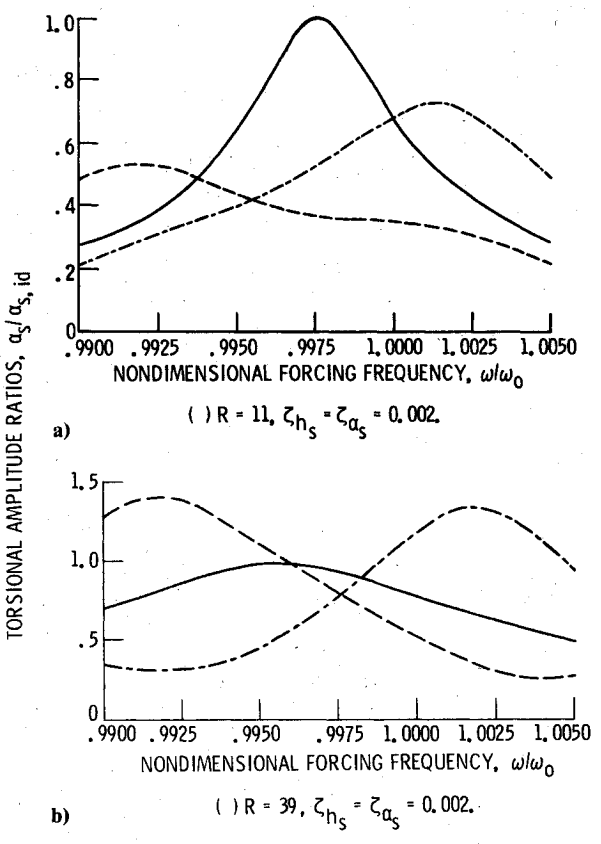

Fig. 11 Effect of blade alternating mistuning on coupled bending-torsion response ($a = 0$, $\omega_{h_s}/\omega_0 = 3.057$, $k = 1.2$, c.g. at midchord, $\zeta_{h_s} = \zeta_{\alpha_s} = 0.002$): a) $R = 11$, b) $R = 39$.

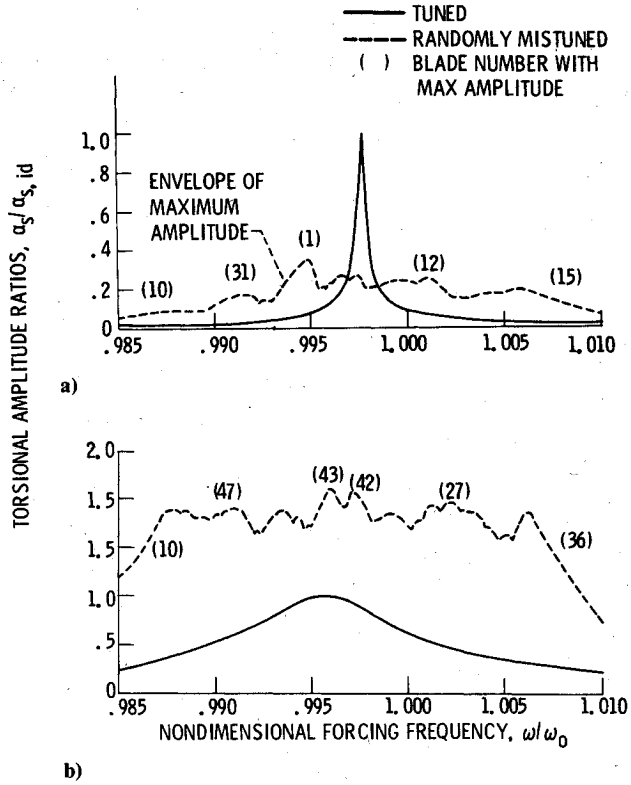

Fig. 12 Effect of blade random mistuning on coupled bending-torsion response ($a = 0$, $\omega_{h_s}/\omega_0 = 0.357$, c.g. at midchord, $\zeta_{h_s} = \zeta_{\alpha_s} = 0$, $k = 1.2$): a) $R = 11$, b) $R = 39$.

response. Thus, this result provides an added incentive for pursuing the use of mistuning as a passive control. The maximum decrease in amplitude with mistuning for $R=11$ is approximately 25% (Fig. 11a). The maximum increase in amplitude with mistuning for $R=39$ is approximately 40% (Fig. 11b).

The randomly mistuned cascade described in Fig. 6 was analyzed for forced response with $k=1.2$. The results are shown in Fig. 12 for $R=11$ and 39. Each blade has a different amplitude and the interblade phase angle varies. It is seen that the single resonance peak for the tuned case is changed into multiple peaks, and different blades peak at different forcing frequencies. As in the alternating mistuning case, this type of mistuning has a beneficial effect on the $R=11$ excitation. For the $R=39$ excitation, the sharp resonance peak of the tuned system is eliminated. However, for most of the values of the forcing frequency, the mistuned response is higher than the tuned response.

Conclusions

This investigation was conducted in an attempt to improve the basic understanding of the effects of mistuning on aeroelastic stability and response and then to explore the feasibility of using mistuning as a passive control to increase flutter speed and to minimize response. The following conclusions are reached on the basis of the limited results obtained by using incompressible unsteady cascade aerodynamic theory for two types of mistuning:

1) In general, the mistuning has a beneficial effect on the coupled bending-torsion flutter speed. The flutter speed increases monotonically with an increase in alternating blade mistuning level. However, when the mistuning level is about 5% and more, the additional benefit is modest.

2) The inherent random mistuning which exists in real fan, compressor, and turbine stages has a significantly beneficial effect on flutter. This observation is qualitatively in agreement with the experimental results published in the literature.

3) As expected, the effect of structural damping on flutter speed is stabilizing. However, in the presence of mistuning this effect is not as significant as in the tuned case.

4) The use of uncoupled torsional flutter analysis to deduce the effect of elastic axis position was found to be unreliable because the coupling between bending and torsion, structural damping, and mistuning can change the results significantly.

5) Mistuning may have either a beneficial or an adverse effect on forced response, depending on the engine order of excitation.

6) Mistuning introduced multiple resonant peaks for a given engine order excitation.

References

[1] Cardinale, V. M., Bankhead, H. R., and McKay, R. A., "Experimental Verification of Turboblading Aeromechanics," Paper presented at AGARD 56th Symposium on Turbine Engine Testing, Torino, Italy, Sept.-Oct. 1980.

[2] Srinivasan, A. V. and Frye, H. M., "Effects of Mistuning on Resonant Stresses of Turbine Blades," Paper presented at ASME Winter Annual Meeting, New York, Dec. 1976.

[3] Whitehead, D. S., "Torsional Flutter of Unstalled Cascade Blades at Zero Deflection," Aeronautical Research Council, R&M 3429, 1965 (S&T Memo 12/63, ARC 26085).

[4] Whitehead, D. S., "Effect of Mistuning on the Vibration of Turbomachine Blades Induced by Wakes," *Journal of Mechanical Engineering Science,* Vol. 8, No. 1, 1966, pp. 15-21.

[5] Hanamura, Y. and Tanaka, H., "A Modification of Flutter Characteristics by Changing Elastic Nature of Neighboring Blades in Cascades," Paper 50 presented at 1977 Tokyo Joint Gas Turbine Congress, Japan, May 22-27, 1977.

[6] Ewins, D. J., "An Experimental Investigation of the Forced Vibration of Bladed Disks Due to Aerodynamic Excitation," Paper presented at ASME Winter Annual Meeting, New York, Dec. 1976.

[7] Srinivasan, A. V., "Influence of Mistuning on Blade Torsional Flutter," NASA CR-165137, Aug. 1980.

[8] Shiori, J., "Non-Stall Normal Mode Flutter in Annular Cascades, Part II: Experimental Study," *Transactions of Japan Society of Aeronautical Engineering,* Vol. 1, 1958, p. 26.

[9] Carta, F. O., "Coupled Blade-Disk-Shroud Flutter Instabilities in Turbo-jet Engine Rotors," *Journal of Engineering for Power,* Vol. 89, 1967, pp. 419-426.

[10] Rao, B. M. and Kronenburger, L., Jr., "Aeroelastic Characteristics of a Cascade of Blades," Texas A&M Research Foundation, College Station, Rept. AFOSR-TR-78-1027, Feb. 1978 (AD-A055 619/IGA).

[11] Bendikson, O. and Friedman, P., "Coupled Bending-Torsion Flutter in Cascades," *AIAA Journal,* Vol. 18, Feb. 1980, pp. 194-201.

[12] Whitehead, D. S., "Force and Moment Coefficients for Vibrating Airfoils in Cascades," Aeronautical Research Council, R&M 3254, Feb. 1960.

[13] Smith, G. C. C. and Elchuri, V., "Aeroelastic and Dynamic Finite Element Analyses of a Bladed Shrouded Disk," NASA CR-159728, March 1980.

[14] Kielb, R. E. and Kaza, K. R. V., "Aeroelastic Characteristics of a Cascade of Mistuned Blades in Subsonic and Supersonic Flows," Paper 81-DET-122 presented at 8th Biennial ASME Engineering Division Conference on Mechanical Vibration and Noise, Hartford, Conn., Sept. 1981.

[15] Lane, F., "System Mode Shapes in the Flutter of Compressor Blade Rows," *Journal of the Aeronautical Sciences,* Vol. 23, Jan. 1956, pp. 54-56.

[16] Dugundji, J., "Flutter Analysis of a Tuned Rotor with Rigid and Flexible Disks," GT&PDL Rept. 146, MIT, Cambridge, Mass., July 1979.

[17] Bisplinghoff, R. L. and Ashley, H., *Principles of Aeroelasticity,* John Wiley & Sons, New York, 1962.

[18] Smith, S. N., "Discrete Frequency Sound Generation in Axial Flow Turbomachines," Aeronautical Research Council, R&M 3709, 1973.

[19] Adamczyk, J. J. and Goldstein, M. E., "Unsteady Flow in a Supersonic Cascade with Subsonic Leading Edge Locus," *AIAA Journal,* Vol. 16, Dec. 1978, pp. 1248-1254.

[20] Moore, D. R. and Reid, R., "Performance of a Single-Stage Axial-Flow Transonic Compressor Stage with a Blade Tip Solidity of 1.7," NASA TM X-2658, Dec. 1972.

[21] Nabatova, N. A. and Shipov, R. A., "Influence of the Material of the Rotor Blades of an Axial-Flow Compressor under Flutter Initiating Conditions," translated from *Problemv-Prochnostl,* No. 8, Aug. 1974, pp. 63-67.